Frequency Dependent Attenuation of Oscillations in Fluid-filled Pipes and Orifices

J. Koreck[1], O. von Estorff[2]

[1] *Robert Bosch GmbH, Stuttgart, Germany, Email: juergen.koreck@de.bosch.com*

[2] *Institute of Modelling and Computation, TU Hamburg-Harburg, Germany, Email: estorff@tu-harburg.de*

Introduction

Gasoline direct injection systems are characterized by a high system pressure and high valve dynamics. Therefore oscillating pressure pulsations and waterhammer phenomena are common effects. In the view of acoustics an extended modelling approach is required in order to capture all physical effects.

In general, such hydraulic systems, including pipes, diameter changes, orifices and volume chambers, are modelled by a 1D approach, and steady state pipe friction, being well established and validated, is assumed. But oscillating pressure pulsations and waterhammer effects need to be modelled with unsteady frequency dependent attenuation, which has approved solutions in time and frequency domain. This is necessary because the damping mechanisms directly influence the quantitative prediction of the fluid sound level and therefore all other depending acoustic quantities.

But common frequency domain approaches so far do not account for flow-related effects. Even in the case of no mean flow, oscillating pressure pulsations create nonlinear velocity dependent resistance at orifices and diameter changes. In the case of high frequency oscillations, the steady state orifice law according to Bernoulli underestimates real effects. Therefore the unsteady orifice behaviour is investigated. Further on the limits of validity of the no flow assumption are inspected with an experimental setup and compared to published results.

Steady and Unsteady pipe friction

A constant pressure gradient Δp along the axis of a circular pipe filled with an incompressible fluid, results in the well-known Hagen-Poiseuille flow which implies a parabolic velocity distribution. This results in the steady state resistance per length in the case of laminar flow

$$R' = \frac{8\mu}{\pi r^4}, \tag{1}$$

where μ is the dynamic viscosity and r is the radius of the pipe.

In unsteady laminar flow the pressure gradient is time dependent. The velocity distribution is no longer parabolic because the viscous effect is concentrated in a thin layer close to the pipe wall. The thickness

$$d_v = \sqrt{\frac{2\pi\upsilon}{\omega}} \tag{2}$$

of this viscous boundary layer depends on the kinematic viscosity v and the angular frequency ω. If the acoustic wavelength is large compared to the radius and large compared to the boundary layer thickness, the series impedance based on unsteady frequency dependent friction is

$$Z = \frac{J_0(ir\sqrt{i\omega/\upsilon})}{J_2(ir\sqrt{i\omega/\upsilon})} i\omega L', \tag{3}$$

where J_0 is the Bessel function of first kind, zeroth order and J_2 is the Bessel function of first kind, second order. With the fluid density ρ and the orifice area A the per length inertance is defined as

$$L' = \frac{\rho}{A}. \tag{4}$$

The series impedance in general is given as

$$Z = R' + i\omega L'. \tag{5}$$

Therefore the per length resistance of the unsteady frequency dependent friction is calculated by taking the real part of equation 3.

The resistance and impedance values can directly be implemented in the transfer matrix method (TMM). An overview of this method for distributed pipe elements with different friction models is given in [1]. The TMM uses a transfer matrix to create the relation between two input parameters and two output parameters in the frequency domain. In hydraulics the in- and output variables are in terms of pressure and flow rate.

Orifice Law

The steady state Bernoulli equation is described by the equation

$$q = c_d A \sqrt{\frac{2\Delta p}{\rho}}, \tag{6}$$

where q is the volume flow and c_d is the discharge coefficient. For low Reynolds numbers the discharge coefficient increases with the Reynolds number while for high Reynolds numbers the discharge coefficient reaches a constant value of about 0.7. Following [2] the orifice resistance is evaluated as

$$R = \frac{1}{{c_d}^2}\frac{\rho}{A^2}q\,, \qquad (7)$$

where the discharge coefficient is constant. For further calculations in this work the dimensionless loss parameter σ is used to replace $1/c_d^2$.

Measurement Setup

Figure 1 depicts the geometry of the test case presented in this work. It consists of two pipes joined by an orifice and filled with water. The pipes have an inner diameter of 4.6mm. The length of the first pipe is 250mm while the length of the second one is 300mm.

The experimental setup uses two axisymmetric piezo actuators to generate a flow excitation at the inlet of the specimen. The voltage signal that activates the actuators follows a sine-sweep up to several kilohertz. The measurement procedure is explained in more detail in [4].

The pressure pulsations are measured at the inlet and the closed end. The transfer function is evaluated from those two signals. The damping ratio is evaluated from the transfer function through curve fitting at the eigenfrequencies.

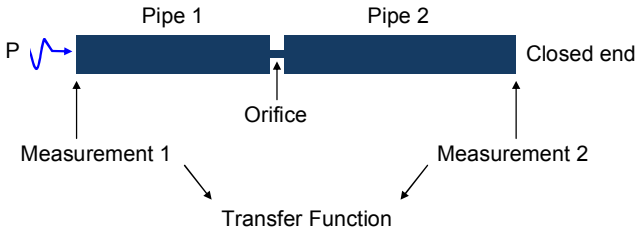

Figure 1: The investigated test case consisting of three fluid columns.

Experimental Results

First of all a simple pipe of total length 550mm is investigated, where no orifice is present. The resulting transfer function is compared to the result of the TMM with unsteady frequency dependent friction in Figure 2. The amplitudes at the eigenfrequencies of the measured transfer function are lower than the calculated ones. This is especially true for the first two peaks. On the other side the eigenfrequencies fit very well. The minor deviations at 1.5 kHz and 5 kHz are a result of structural resonances. From the transfer function the damping ratio is evaluated at every peak. This is done by analyzing the peakwidth of the half power points of each single mode. The resulting damping ratios are plotted in Figure 3. Of course the damping ratios of the TMM are exactly on the theoretical values. The damping ratios of the measurement are close to the TMM values. The first mode shows the biggest deviation, which is also true for all succeeding measurements. Due to this systematic deviation, the first mode is not considered in the final evaluation. The damping ratio of the third mode fits the predictions quite well, while the results of the fourth to the seventh mode show slightly increased values. Between 8 and 9 kHz the measurement setup starts to show the influence of the actuator

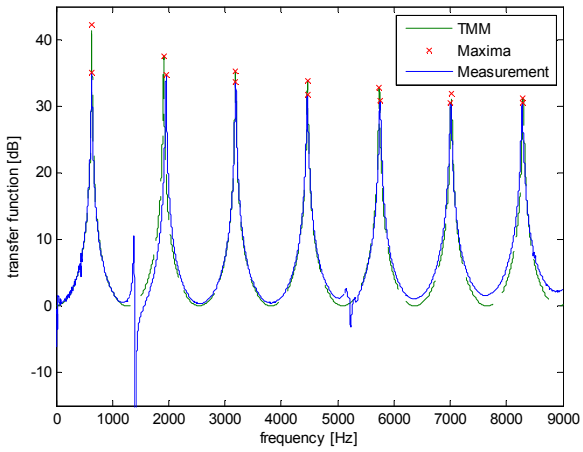

Figure 2: Calculated and measured transfer function for the simple pipe.

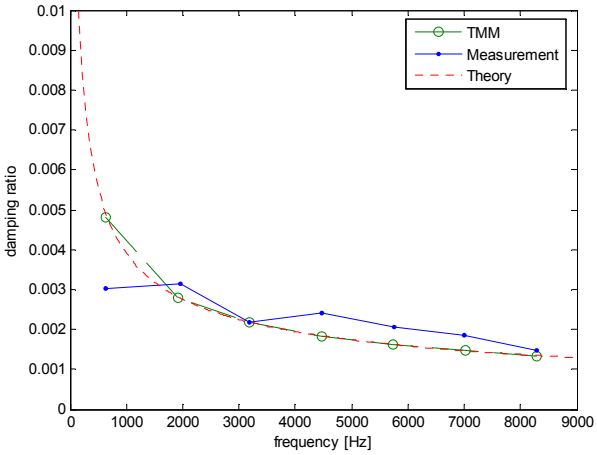

Figure 3: Damping ratios evaluated from the calculated and measured transfer function of the simple pipe.

eigenfrequency. Therefore only the first seven eigenfrequencies are taken into account.

In the next step a circular orifice with sharp edges is built between two pipes, which correspond to the test case described in the previous section. Here the orifice is 2 mm long and has a diameter of 1.2 mm. Figure 4 shows the corresponding transfer function. Again the eigenfrequencies fit quite well except for the one at 8 kHz, while the peak heights of the measurements are lower than the TMM calculations. The damping ratios are depicted in Figure 5. Certain modes of the TMM results show a higher damping ratio than the simple pipe. This is because the higher local attenuation of the fluid column in the orifice applies at a position of a high pressure gradient. In this setup, those are the modes with uneven numbers. Modes with even numbers have almost the same eigenfrequency and damping ratio as in the case with the simple pipe. Again the first mode of the measurement has an unrealistic low value for the damping ratio. Over all modes the measurements show a higher damping ratio as the TMM. This results from the additional velocity dependent resistance in the orifice, which is explained in the next section. The difference between even and uneven modes remains visible in the measurements.

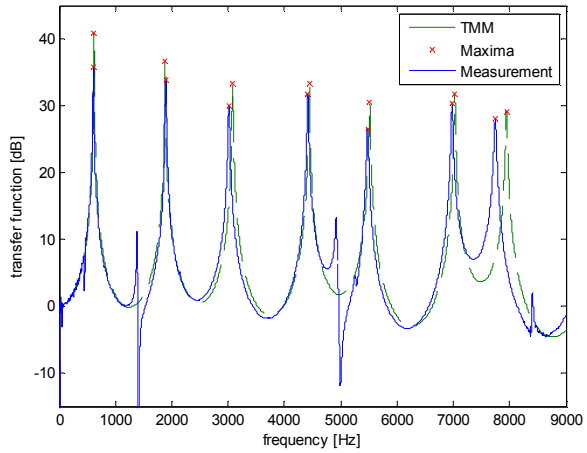

Figure 4: Calculated and measured transfer function for the test case with a 1.2x2mm orifice.

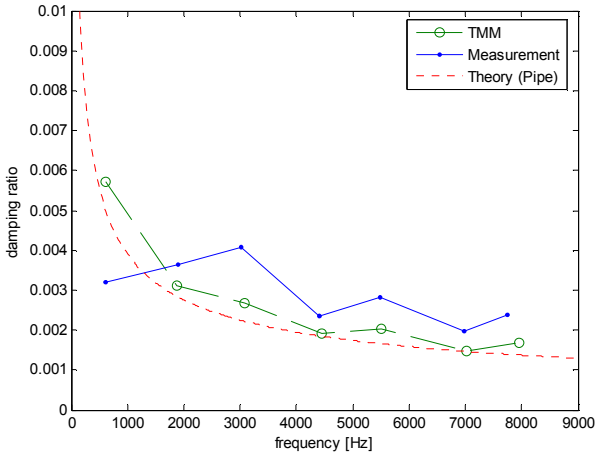

Figure 5: Damping ratios of the TMM and the measurements for the test case with a 1.2x2mm orifice.

Now the influence of the excitation level is investigated. An orifice with a diameter of 0.9mm and a length of 2mm in the test case shows a clear influence of the pressure excitation. Figure 6 and Figure 7 show the transfer functions and damping ratios, respectively. Again the uncertainty for the first mode is very high. The third and the fifth mode show a clear influence of the excitation level. The test case with orifice compared to the simple pipe attenuates especially the uneven modes. A variation of the excitation level also leads to an increased attenuation of the uneven modes. Clearly the standard TMM is not capable to account for a change in excitation level.

Velocity Dependent Resistance in TMM

The TMM so far is only capable to account for the frequency dependent friction. In order to account for the Bernoulli effect in the frequency domain, the resistance from equation 7 is added to the resistance resulting from the unsteady viscous boundary layer. Therefore the resistance becomes dependent on the amplitude of the velocity in the orifice. But the velocity in the orifice also depends on the resistance of the orifice. Hence the TMM must be solved iteratively. There is only one valid parameter combination per frequency.

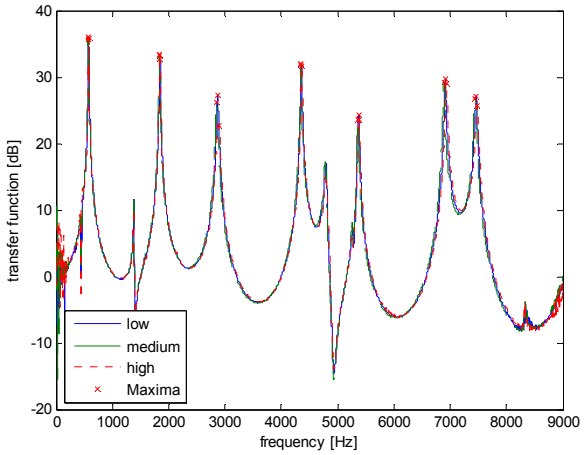

Figure 6: Experimental transfer function for a variation of the excitation level for the test case with a 0.9x2mm orifice.

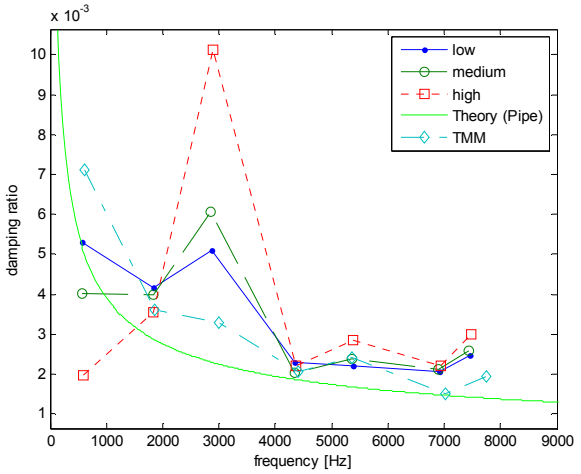

Figure 7: Damping ratios of the TMM and the measurements for the test case with a 0.9x2mm orifice.

Figure 8 depicts the procedure, which calculates the damping ratio from the input pressure and a given discharge coefficient. With this approach it is possible to compare the quasi-steady orifice law and a fit to the experimental results. The quasi-steady orifice law assumes a constant value for the loss coefficient σ in the resistance equation of the orifice. The experimental fit uses an optimization routine to find the σ values for the single measurements. Besides the geometry and the material properties the optimization algorithm needs the experimental input pressure in the frequency domain and the damping ratio of the third mode.

Evaluation of Results

The results from this approach are depicted in Figure 9. For the quasi-steady orifice law the loss coefficient σ is 2 while it increases from 1.9 to 2.3 and 4.0 with the orifice velocity for the experimental fit calculation. In the case of the lowest excitation level the damping ratio as well as the velocity in the orifice agree very well. For higher excitation levels the damping ratio is too low as well as the velocity amplitude in the orifice is too high compared to the experimental fit calculations.

For low orifice velocities the resistance due to Bernoulli becomes negligible. Therefore only the resistance from the

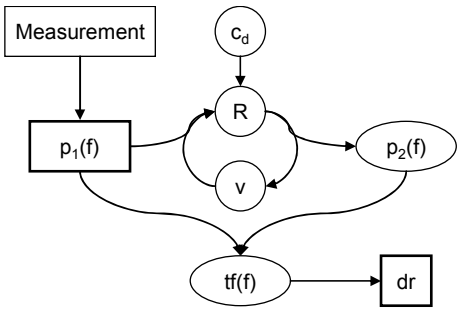

Figure 8: TMM with velocity dependent resistance of the orifice, where tf is the transfer function and dr is the damping ratio.

viscous boundary layer is important, which is also depicted in Figure 9. The velocity range for which this statement is approximately true, is an important question for the choice of the appropriate and efficient calculation tool. In the present case the low velocity approximation is plotted as far as 0.4 m/s. This results from a statement made by [5]. Here a non-dimensional orifice velocity of 3 is used to separate the linear form the nonlinear behaviour. The non-dimensional orifice velocity is calculated by dividing the regular orifice velocity by $\sqrt{\nu\omega}$. This statement is made on the basis of correlation of published experimental data for thin orifices ($l/d \rightarrow 0$). In the present case the length to diameter ratio is 2.22.

Further on the nonlinear region ranges from a non-dimensional velocity value of 3 to 100 [5]. Here the transition from no velocity dependence to a more or less linear dependence is noticed. Above a value of 100 the resistance is roughly linear with the velocity. As shown in the work of [6] the frequency dependence is gradually lost between values of 3 and 100 for the non-dimensional orifice velocity. But the range of measurements with very high orifice velocities is not wide enough to make a clear statement about the quasi-steady behaviour [5].

An increase of σ with the orifice velocity is also recognized in [3]. At high velocities in the orifice σ seems to reach a maximum. In order to compare the experimental results of this work to the statements made in [5], the non-dimensional velocity is calculated. It ranges from 3.7 to 6.8 for the results of the experimental fit depicted in Figure 9.

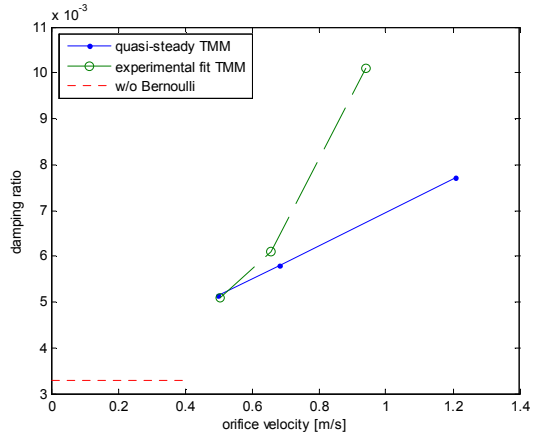

Figure 9: Damping ratio of the third mode plotted over orifice velocity for different calculation schemes (test case with 0.9x2mm orifice).

Conclusion

A method to evaluate the effect of unsteady pipe friction and unsteady orifice resistance is presented. Velocity dependent resistance is added to the standard TMM modelling approach.

Following [5] the resistance of orifices can be divided into three velocity ranges. For very low orifice velocities only the unsteady pipe friction in the orifice is important and the resistance is therefore frequency dependent. For high orifice velocities the resistance seems to depend only on the velocity. In the medium range the influence of the frequency dependent friction decreases while the velocity dependent resistance becomes more important.

This nonlinear region is investigated in this work. So far the resistance due to unsteady pipe friction is added to the resistance due to velocity dependent orifice friction.

According to the measurements and the calculations the loss coefficient in unsteady flow increases with the velocity amplitude in the orifice. The values for the loss coefficient in unsteady flow are higher than common values for steady state conditions.

Measurements of additional geometries could improve the knowledge in a wider orifice velocity range. Furthermore the low and high velocity approximations could be investigated in the future.

Acknowledgements

The authors wish to thank Dipl.-Ing. Jan Herrmann of the Institute of Applied and Experimental Mechanics, University of Stuttgart for his support with the measurement setup.

References

[1] J. Watton: Modelling, Monitoring and Diagnostic Techniques for Fluid Power Systems. Springer, London, 2007

[2] D.N. Johnston, K.A. Edge: The impedance characteristics of fluid power components. Proceedings of the Institute of Mechanical Engineers **205** (1991), 3-10

[3] G.B. Thurston, L.E. Hargrove, B.D. Cook Jr.: Nonlinear Properties of Circular Orifices. Journal of the Acoustical Society of America **29** (1957), 992-1001

[4] J. Herrmann, M. Spitznagel, L. Gaul: Fast FE-analysis and measurement of the hydraulic transfer function of pipes with non-uniform cross section. NAG/DAGA 2009, Rotterdam, Netherlands

[5] R.L. Panton, A.L. Goldman: Correlation of nonlinear orifice impedance. Journal of the Acoustical Society of America **60** (1976), 1390-1396

[6] G.B. Thurston, C.E. Martin Jr.: Periodic Fluid Flow through Circular Orifices. Journal of the Acoustical Society of America **25** (1953), 26-31